Wind and Structures, Vol. 10, No. 6 (2007) 543-554
DOI: http://dx.doi.org/10.12989/was.2007.10.6.543

Experimental studies on possible vortex shedding in a suspension bridge. Part I – Structural dynamic characteristics and analysis model

S. S. Law†

Civil and Structural Engineering Department, Hong Kong Polytechnic University, Hong Kong, People's Republic of China.

Q. S. Yang‡

Bridge Engineering Department, Beijing Jiao Tung University, People's Republic of China.

Y. L. Fang‡

Mechanical Engineering Department, Tai Yuen University, People's Republic of China.
(Received November 3, 2006, Accepted November 11, 2007)

Abstract: The suspension bridge is situated in an area of complex topography with both open sea and overland turbulence characteristics, and it is subject to frequent typhoon occurrences. This paper investigates experimentally the possible vortex shedding events of the structure under high wind and typhoon conditions. A single-degree-of-freedom model for the vibration of a unit bridge deck section is adopted to determine the amplitude of vibration and to estimate the parameters related to the lifting force in a vortex shedding event. The results of the studies are presented in a companion paper (Law, *et al*. 2007). In this paper, statistical analysis on the measured responses of the bridge deck shows that the vibration response at the first torsional mode of the structure has a significant increase at and beyond the critical wind speed for vortex shedding as noted in the wind tunnel tests on a section model of the structure.

Keywords: wind; typhoon; dynamic; vortex shedding; suspension bridge; steel; traffic; model; optimization.

1. Introduction

Vortex shedding is characterized with the fluctuating lift force on the obstacle. Existing theoretical predictions have the following basic assumptions: a) the structure on which the air flow sweeps is a one dimensional body; b) the structure is a transversely rigid body and is supported elastically; and

† Associate Professor, Corresponding Author, E-mail: cesslaw@polyu.edu.hk
‡ Professor

c) the airflow is steady and smooth. In the analysis of a segment of a structure, it is generally assumed that the vortex-induced excitation is uniform along the segment length.

The different models proposed previously for vortex shedding study can be categorized according to the method to model the lift coefficients. They are the coupled lift-oscillator models and the single-degree-of-freedom (SDOF) models. The fluid-body system is represented by two differential equations in the first group of models where the periodic wake of the body is treated as an oscillator. Previous investigators attempted to simulate the wake-body behaviour through judicious choice of the coefficients and the form of coupling between the two oscillators (Harlten and Currie 1970, Skop and Griffin 1975, Iwan and Blevins 1974, Billah 1989). In the SDOF model, a single equation of motion is used to represent all the mechanisms of vortex-induced vibration through expressing the lift force as a polynomial function of the instantaneous motion of the body (Sarpkaya 1978, Vickery and Basu 1983, Staubli 1983, Simiu and Scanlan 1996). Both groups of models are empirical while the SDOF models are used extensively in the response amplitude prediction (Goswami, *et al*. 1993a).

Much effort has been spent on finding a suitable expression for the lifting force that fits the experimentally observed data. There is a variety of approaches to construct the empirical dimensionless lift force coefficients. But contrasting to the relative ease in constructing the equation of motion, it is difficult to identify the lift force coefficients. Models based on different kinds of response measurements are proposed. Christensen and Roberts (1998) proposed a general SDOF model in which the coefficients of the lift force can be identified recursively by processing the digitized records of the dynamic responses.

The bridge is situated in an area of complex topography with both open sea and overland turbulence characteristics, and it is subject to frequent typhoon occurrences averaging between two and three times a year. Predictions on the behaviour of the structure under wind load have been made as part of the design requirements. It is known that galloping, torsional divergency and flutter are unstable responses which should be avoided in the design, while vortex shedding is frequent and unavoidable.

This paper investigates the possible vortex shedding from statistical analysis on the power spectrum of the responses of the bridge deck at different wind speeds. The measured data collected soon after the completion of deck welded connections of the bridge in 1996 were used. Results indicate the dependence of vibration amplitude at the first torsional mode with wind speed. A SDOF model of the vibration of unit length of the bridge deck section is also presented, and the amplitude of vibration together with the parameters related to the lifting force in a vortex shedding event could then be estimated from the measured structures responses. Results on the application in further studies are reported in a companion paper (Law, *et al*. 2007).

2. The suspension bridge

The suspension bridge has a total length of 2,160 metres, including a main span of 1,377 metres and a suspended span of 355.5 metres at the western side and four non-suspended approach spans of 72 metres each, supported by a series of concrete piers at the eastern end. The structure provides approximately 70 metres clearance from the mean high water level. An elevation view of the bridge is shown in Fig. 1. The hybrid truss/box bridge deck has two carriageways, each of which carries three lanes on its upper deck level for road traffic, and there is a lower deck with two rail tracks and two sheltered emergency lanes for road traffic during high wind conditions. A typical cross-section is shown in Fig. 2. The bridge deck consists of transverse Vierendeel cross-frames supported

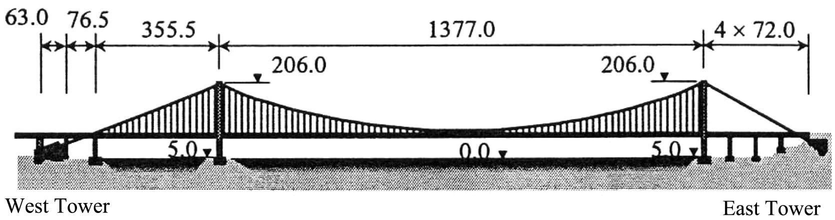

Fig. 1 Elevation of the suspension bridge (dimensions in metre)

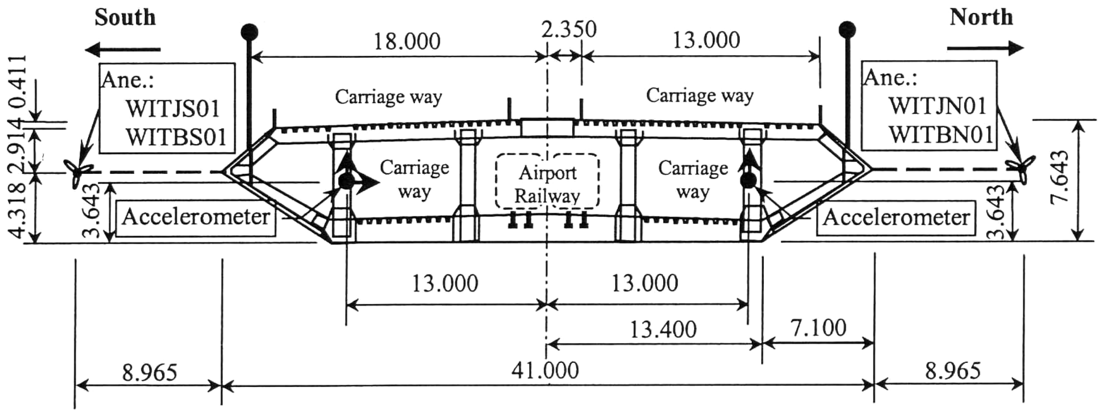

Fig. 2 Cross-section of bridge deck and sensor locations (dimensions in metre)

on longitudinal diagonally braced trusses acting compositely with the stiffened plate carriageway members. The deck structure is continuous between the two main anchorages and is suspended from the main cables at 36 metres spacing.

The natural frequencies of the completed structure after completion of the welding of the deck connections have been measured and the first 19 natural frequencies are reproduced in Table 1. The mode shapes of the first four lateral modes, the first four vertical modes and the first two torsional modes are shown in Fig. 3.

3. Wind tunnel test results

Wind tunnel tests on sectional models of the suspension bridge deck have been conducted and the aerodynamic stability arising from vortex shedding vibration was investigated in different studies. Since it was generally not possible to adequately reproduce the turbulence properties of the natural wind, the testing was therefore performed in smooth flow. The critical wind speeds obtained from testing are therefore only quoted for the smooth flow condition. This sectional model measurement in smooth flow tends to overestimate vortex shedding amplitudes. The investigation has been carried out based on the measurement of the aeroelastic responses. The design wind speeds were based upon the one minute mean wind speed. In the study of vortex shedding responses, a typical time for 10 cycles of vibration was considered necessary to attain a steady state amplitude, and only vortex shedding with the second vertical and first torsional modes was studied with an averaging time of the order of 72 seconds for the bending mode and 37 seconds for the torsional mode.

In the design of the bridge structure, the critical wind speeds for vortex shedding oscillation in the

Table 1 Natural Frequencies and nature of mode shape of the suspension bridge after completion of welding

Mode Order	Natural Frequency (Hz)		Mode Shape description
	Computed	Measured	
1	0.068	0.069	1st lateral
2	0.117	0.113	1st vertical
3	0.137	0.139	2nd vertical
4	0.158	0.164	2nd lateral
5	0.189	0.184	3rd vertical
6	0.210	0.214	3rd lateral
7	0.230	0.226	4th lateral
8	0.232	0.236	5th lateral
9	0.240	0.240	6th lateral
10	0.245	0.241	4th vertical
11	0.271	0.267	1st torsional
12	0.294	0.284	5th vertical
13	0.285	0.297	7th lateral
14	0.311	0.320	2nd torsional
15	0.325	0.327	6th vertical
16	0.333	0.336	8th lateral
17	0.340	0.352	9th lateral
18	0.365	0.381	10th lateral
19	0.367	0.347	11th lateral

second vertical bending mode and the first torsional mode are 7.44 m/s and 13.57 m/s respectively. The wind tunnel test results showed that bending oscillations at the second vertical modal frequency of 0.137 Hz occurred when the wind speed was in the range 6.9 m/s to 9.4 m/s. And torsional oscillations at the first torsional modal frequency of 0.25 Hz occurred when the wind speed was in the range 12.2 m/s to 19.9 m/s. The critical wind speeds from both the design and wind tunnel test are close to each other. The test results showed that the deck is basically stable at 0^o and positive values (wind from below the deck) of wind incidence, under the condition of no traffic and trains. They however showed a vortex response at negative values and higher positive values of wind incidence. Vortex shedding does occur under the condition with traffic and trains. The vortex shedding amplitudes are however high, ranging from 19 mm to 278 mm in bending and 36 mm to 800 mm in torsion, and the results are reproduced in Table 2 for comparison with results from this study. It is noted that the amplitude of vibration in the torsional mode is referred to that at the edge of the bridge deck.

4. Experimental study soon after completion of deck welding

4.1. Field measurement

The measurements were made soon after the completion of welding of deck connections of the

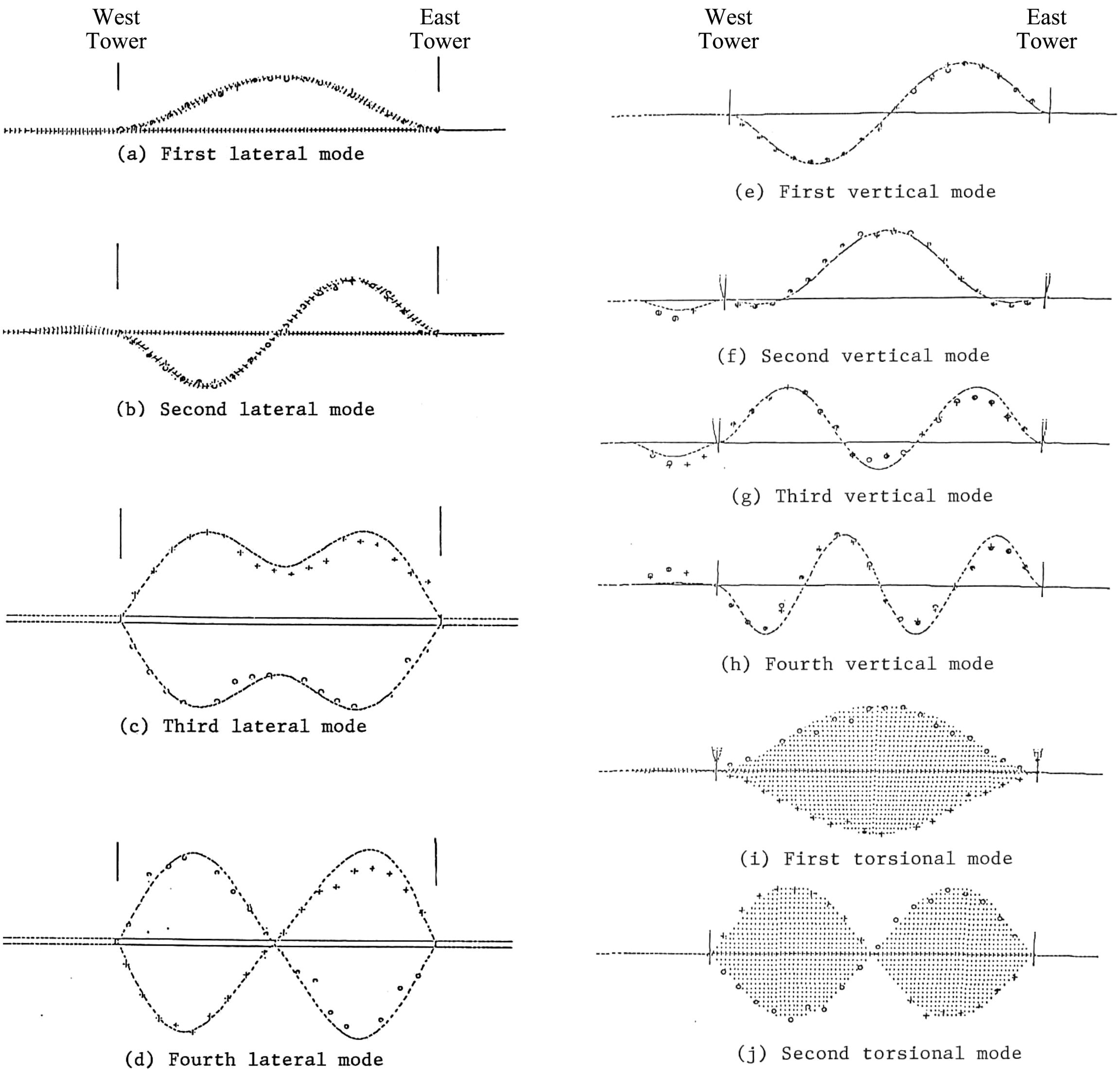

Fig. 3 Vibration mode shapes (+, o measurement points)

bridge deck, and the bridge deck behaved as an integral structure suspended from the cables. Accelerometers were installed on both the cables and the bridge deck at Section *J* (Fig. 4) to monitor most of the vibration modes. They were installed in three orthogonal directions parallel and perpendicular to the bridge deck. Accelerometers placed inside the bridge deck are located close to the horizontal centroidal axis of the deck section below the suspender. The accelerometers are of model KYOWA ASQ-1BL, servo type. One THIES Model 4.3323.32.012 m anemometer was installed on top of a two metre high steel post tied securely to a permanent vertical post on top of the deck for monitoring both the horizontal wind speed and direction. The location of the anemometer was selected away from existing temporary fixtures and machines on top of the deck. The signals collected were recorded by an analogue tape recorder KYOWA RTP-800A, and they were later

Table 2. Wind tunnel test results on vortex shedding

Angle of wind incidence	Bending (Damping = 0.03)		Torsion (Damping = 0.03)	
	Wind Speed (m/s)	RMS amplitude (mm)	Wind Speed (m/s)	RMS amplitude (mm)
-7.5°	7.1/7.4	134/252	13.4/15	231/443
-5.0°	6.9/7.8	25/169	12.2/15.6	331/143
-2.5°	-/8.1	Stable/20	13.1/16.8	162/336
0°	-/9.3	Stable/19	-/18.5	Stable/442
+2.5°	9.4	278/Stable	13.8/19.9	36/747
+5.0°	-/9.3	Stable/208	-/19.9	Stable/800
+7.5°	-/9.3	Stable/24	-/19.5	Stable/668

Note: */* indicates the value without and with traffic and trains.

digitized using GLOBALAB package and DATA TRANSLATION A/D Board DT2829 at 1 Hz. The recording started at 11:23 and ended at 18:13 on 22 July 1996 with a four minute break. Both the wind and acceleration data were obtained from this measurement.

The weather was sunny in the morning. Typhoon signal No. 1 was up in the afternoon to mark the strong monsoon with heavy rain and gust winds as high as 75 km/hr.

4.2. Data analysis

The time history data files are analyzed by computing the moving averages over consecutive 512 second segments of data to capture long sequence of bridge oscillations under wind (Hay 1992). The Fast Fourier Transforms of these segments are then used to describe the dynamic response in the frequency domain.

4.3. Wind characteristics

The data set of the averaged time histories consist of: the wind speed V, horizontal wind direction θ and the wind speed normal to the bridge deck (incident wind speed). The convention for θ is shown in Fig. 4 and it corresponds to the wind coming from a compass bearing of 163.4° (16.6 east of south) when $\theta=0$, and θ is increasing in the same sense as the compass bearing. The moving averages over segments of 512 seconds of the wind speed, the incident wind speed and direction are computed and they are shown in Fig. 5. The data sets cover a seven hour period during which the wind mainly came from the south-east compass quadrant with an average angle of 326° (34° to the normal line). The turbulence intensity of wind is also plotted in Fig. 5, and it is between 0.18 and 0.25 most of the time and is quite high.

4.4. Acceleration characteristics

The acceleration data from the bridge deck was also sorted in segments of 512 seconds into different files according to the selected average wind speed. Those segments corresponding to an average incident wind speed within a 0.5 m/s bandwidth were grouped into a single record. The wind

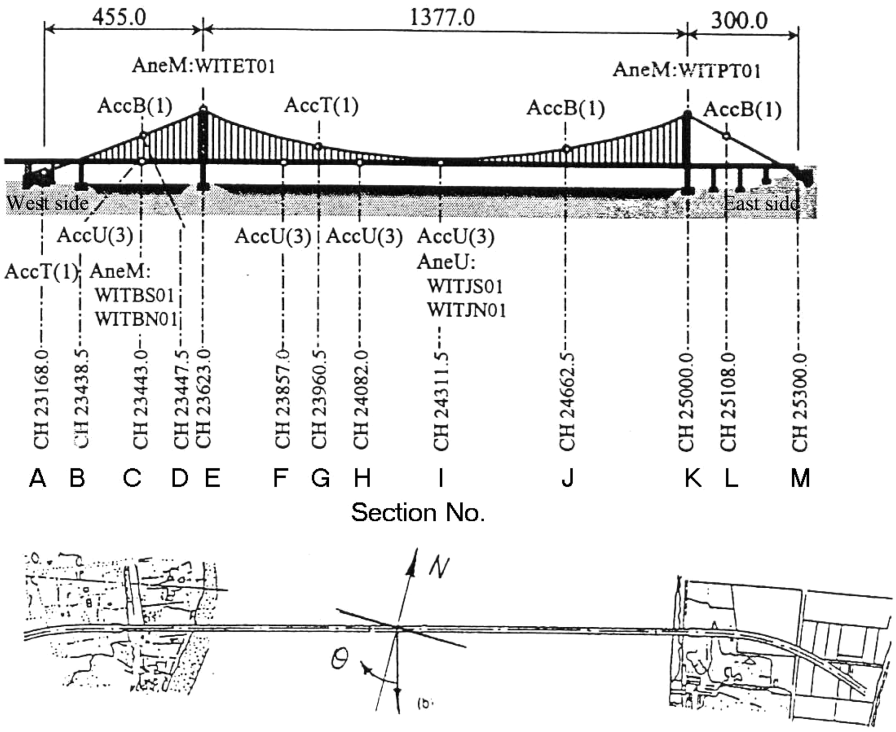

Fig. 4 Location of instruments (dimensions in metre)

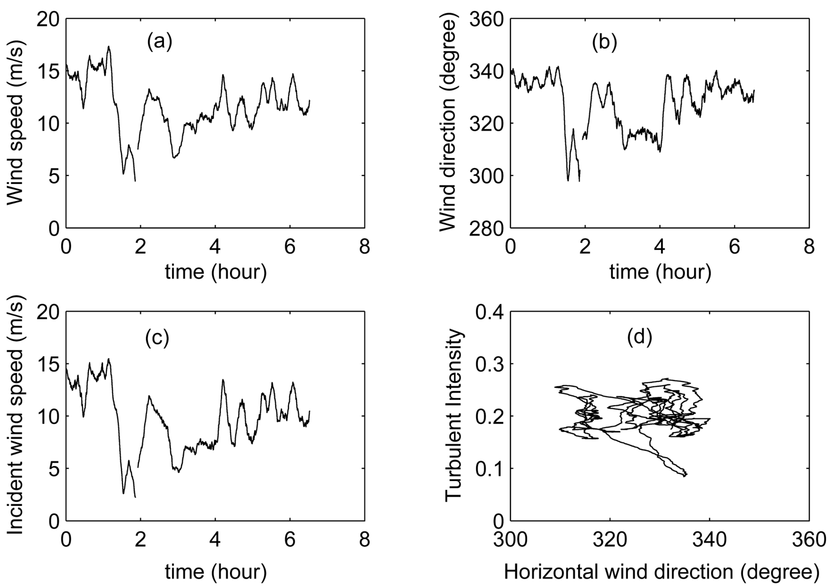

Fig. 5 Average wind characteristic in first study

speeds corresponding to these segments have a maximum standard deviation less than 0.27 m/s. Auto-power spectra of the vibration of the bridge deck at different wind speed were obtained by performing an FFT of size 512 on the sorted vibration records and taking the average of them with a frequency resolution of 0.001953 Hz. The power spectrum is obtained, a sample of which is shown in Fig. 6 for various wind speeds. The spectral amplitude of the first vertical mode at 0.113 Hz has a significant increase from a wind speed of 5 m/s to 9 m/s, while that for the third vertical mode at 0.184 Hz has a large increase at wind speed of 13 m/s as shown in Fig. 6(a). Changes in the second vertical mode and the first torsional mode are not observed because the locations of the sensors are not at the peaks of these mode shapes (Fig. 3). The changes in the vertical spectral peaks are noted to be different from those observed for the lateral modes shown in Fig. 6(b). The spectral amplitudes of the first and second lateral modes increase monotonically with wind speed from 5 m/s to 13 m/s. This is because the bridge deck is under increasing horizontal wind load with increasing wind speed. These observations suggest that the spectral peaks of the vertical and torsional modes are dependent on the wind conditions.

The spectral peak of each vibration mode is again plotted against the average incident wind speed for further study of such dependence, and the graphs are shown in Fig. 7. There is no negative value of mean wind speed so that any dependence under all wind directions cannot be studied. Most of these modes exhibit monotonic increase in amplitude with increasing wind speed.

Both the first vertical mode and first torsional mode exhibit distinct jumps in the amplitude at a wind speed of 13.25 m/s, and this sudden jump amounts to two and three times of the initial value of the two modes respectively. This amplitude increment is maintained over a relatively wide range of wind speed after 13 m/s in the first torsional mode. This observation could only be related to the wind effect, and it also matches the finding from the wind tunnel tests that vortex shedding oscillation will occur at around 13.57 m/s wind speed. However no special observations are made in all the vibration modes at a wind speed close to 7.5 m/s as observed in the wind tunnel tests for the second vertical bending mode.

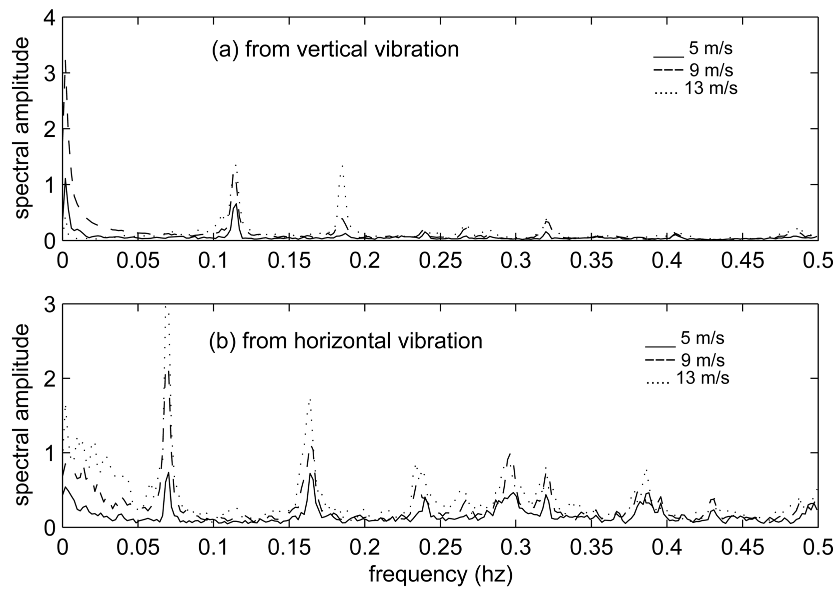

Fig. 6 Auto-power spectrum of vibration at different wind speeds

5. Model for parameter estimation

Before we proceed to the next phase of experimental studies, the mathematical tools we adopted in the analysis are presented and discussed.

The response of a flexible bridge deck is a combination of oscillation components from different frequencies, and usually the lifting force on the deck varies along its length. Ehsan and Scanlan (1990) have proposed an analytical model on vortex shedding of flexible bridges accounting for imperfect correlation of forces along the bridge deck. The formulation carries an implicit assumption that the aerodynamic forces are highly correlated at spanwise locations where the oscillation amplitude is high and vice versa. This assumption is based on the experimental observation that lock-in phenomenon has an organizing effect on the vortex shedding of the structure, leading to greater correlation lengths as the amplitude of vibration for the rigid model is increased. An assumption of uniform lifting forces along the span is therefore made in the present study.

The bridge deck of the suspension bridge is of such a large scale that a segment of it can be modelled as a rigid uniform body suspended elastically such that it can freely vibrate transversely. It is further assumed that the vortex-induced excitation is uniform along the element length with small variation. The suspension can be represented as a linear spring of stiffness k, in parallel with a linear viscous damper, with coefficient c.

When only the transverse motion is under consideration, the governing equation of motion for unit length of the bridge deck segment is

$$\ddot{x} + 2\zeta\omega_n\dot{x} + \omega_n^2 x = \frac{\rho}{2m}U^2 D f(t) \tag{1}$$

and

$$\zeta = \frac{0.5c}{\sqrt{km}};\ \omega_n^2 = \frac{k}{m} \tag{2}$$

and m is the mass per unit length of the segment. ρ is the air density and U is the instantaneous horizontal wind velocity. ζ is the non-dimensional damping, and ω_n is the undamped natural frequency. $f(t)$ is the non-dimensional fluid force. $\rho U^2/2$ is the dynamic pressure and D is the thickness of the bridge deck.

Goswami, *et al.* (1993b) expressed $f(t)$ as a function of the non-dimensional displacement x/D and velocity $\dot{x}/U$ and a vector λ of n parameters. Christensen and Roberts (1998) simplified this expression into a linear-in-the-parameters form as shown below

$$f(t) = \lambda_1\left(\frac{\dot{x}}{U}\right) + \lambda_2\left(\frac{\dot{x}}{U}\right)^3 + \lambda_3\left(\frac{\dot{x}}{U}\right)^5 + \lambda_4\frac{x}{D} \tag{3}$$

The first three terms model the energy dissipation and the last term represents the aerodynamic stiffness. Substituting Eq. (3) into Eq. (1), the equation of motion becomes

$$\ddot{x} + 2\zeta\omega_n\dot{x} + \omega_n^2 x = \frac{\rho}{2m}\left(\lambda_1 DU\dot{x} + \lambda_2 D\frac{\dot{x}^3}{U} + \lambda_3 D\frac{\dot{x}^5}{U} + \lambda_4 U^2 x\right) \tag{4}$$

Eq. (4) can be re-written as

$$\ddot{x} + a_1\dot{x} + a_2\dot{x}^3 + a_3\dot{x}^5 + px = 0 \tag{5}$$

where

$$a_1 = \left(2\zeta\omega_n - \frac{\rho DU}{2m}\lambda_1\right), \qquad a_2 = -\frac{\rho D}{2mU}\lambda_2$$
$$a_3 = -\frac{\rho D}{2mU}\lambda_3, \qquad p = \left(\omega_n^2 - \frac{\rho U^2}{2m}\lambda_4\right) \tag{6}$$

When the responses in a vortex shedding occurrence are available, the method described below can be used to obtain the parameters a_1, a_2, a_3 and p from which the parameters λ_i can be computed.

The state variable filter approach (Gawthrop 1984) is used to estimate the unknown parameters a_i and p. Two parameters c_1 and c_2 are added to both sides of Eq. (5) to get

$$\ddot{x} + c_1\dot{x} + c_2 x = -(a_1 - c_1)\dot{x} - (p - c_2)x - a_2\dot{x}^3 - a_3\dot{x}^5 = -f_1\dot{x} - f_2 x - a_2\dot{x}^3 - a_3\dot{x}^5 \tag{7}$$

with $f_1 = a_1 - c_1$ and $f_2 = p - c_2$. Parameters c_1 and c_2 are filter parameters which are $2\zeta_f\omega_f$ and ω_f^2 respectively and ω_f is the frequency of interest. Parameters c_1 and c_2 can be chosen as any desired value, but they should be positive to guarantee a linear filter, and the pass band of the filter defined by them should encompass the predominant frequencies in the system response.

The right-hand-side of Eq. (7) consists of several types of excitations to the system. The solution to Eq. (7) can be expressed as the sum of

$$x = f_1\dot{y}_1(t) + f_2 y_1(t) + a_2 y_2(t) + a_3 y_3(t) + d_1\dot{y}_4(t) + d_2 y_4(t) \tag{8}$$

for the different types of excitations, and d_1 and d_2 are two additional parameters to allow for non-zero initial conditions. The functions y_i(t) have to satisfy the following differential equations (Gawthrop 1984)

$$\ddot{y}_i + c_1\dot{y}_i + c_2 y_i = v_i(t), \; i = 1,2,3,4 \tag{9}$$

where $v_1(t) = -x(t);\; v_2(t) = -\dot{x}^3(t);\; v_3(t) = -\dot{x}^5(t);\; v_4(t) = 0$.

are the different types of excitations corresponding to the responses y_i(t), and the initial conditions are

$$y_i(0) = \dot{y}_i(0) = 0;\; i = 1, 2, 3. \tag{10}$$
$$y_4(0) = 0; \qquad \dot{y}_4(0) = 1$$

If the initial responses of the system are not zero,

$$w_1 = x(0);\; w_2 = \dot{x}(0) \tag{11}$$

Eqs. (8) to (11) give the values of d_1 and d_2 as

$$d_1 = w_1 = x(0),\; d_2 = w_2 + w_1 c_1 + w_1 f_1 \tag{12}$$

Substituting Eq. (12) into (8), we have

$$x = f_1(\dot{y}_1 + w_1 y_4) + f_2 y_1 + a_2 y_2 + a_3 y_3 + w_1\dot{y}_4 + (w_2 + w_1 c_1)y_4 \tag{13}$$

The parameter identification problem becomes a least squares problem as

$$min\ J = \sum_{i=0}^{N}\{x_i - [f_1(\dot{y}_{1i} + w_1 y_{4i}) + f_2 y_{1i} + a_2 y_{2i} + a_3 y_{3i} + w_1\dot{y}_{4i} + (w_2 + w_1 c_1)y_{4i}]\} \tag{14}$$

where the responses x_i are measured at times t_i. Parameters f_1, f_2, a_2 and a_3 are obtained from Eq.

(14). We can have the coefficients λ_i of the wind force in terms of the damping and stiffness parameters I_i from Eq. (6) as

$$\begin{aligned}
\lambda_1 &= \frac{m}{\rho D} I_1; \quad I_1 = \frac{2}{U}(2\zeta\omega_n - c_1 - f_1) \\
\lambda_2 &= \frac{m}{\rho D} I_2; \quad I_2 = -2Ua_2. \\
\lambda_3 &= \frac{m}{\rho D} I_3; \quad I_3 = -2U^3 a_3. \\
\lambda_4 &= \frac{m}{\rho D} I_4; \quad I_4 = \frac{2}{U^2}(\omega_n^2 - c_2 - f_2).
\end{aligned} \tag{15}$$

6. Solution algorithm

The excitations $v_i(t)$ in Eq. (9) are computed from the measured responses. The differential equation in Eq. (9) is expressed into a state space equation, and the recursive method proposed by Tan and Yang (1995) is used to solve the time functions $y_1, \dot{y}_1, y_2, y_3, y_4, \dot{y}_4$ in Eq. (9). They are then substituted into Eq. (13) to obtain the total response. The parameters f_1, f_2, a_2 and a_3 are then obtained from Eq. (14) as a least squares optimization problem using the MATLAB optimization toolbox. Parameters I_1 to I_4 and the coefficients λ_i are then computed from Eq. (15) when the physical parameters of the bridge deck are available.

7. Conclusions

Statistical analysis on the measured responses of the suspension bridge deck shows that there is a significant increase in the vibration response at the first torsional mode of the structure at and beyond the critical wind speed and this observation matches the findings in the wind tunnel tests. This indicates the dependence of vibration amplitude of this mode with wind speed. A SDOF model of the vibration of a unit length of the deck is presented to determine the amplitude of vibration and to estimate the parameters related to the lifting force in a vortex shedding event. Results from application of the model to possible vortex shedding events will be presented in a companion paper (Law, *et al*. 2007).

Acknowledgements

The work described in this paper was supported by a grant from the Hong Kong Polytechnic University Research Funding Project No. G-S571.

References

Billah, K. Y. R. (1989), "A study of vortex-induced vibration", PhD dissertation, Princeton University, Princeton, N.J.

Christensen, C. F. and Roberts, J. B. (1998), "Parametric identification of vortex-induced vibration of a circular cylinder from measured data", *J. Sound Vib*, **211**(4), 617-636.

Ehsan, F. and Scanlan, R. H. (1990), "Vortex-induced vibration of flexible bridges", *J. Eng. Mech.*, ASCE, **116**(6), 1392-1410.

Gawthrop, P. J. (1984), "Parametric identification of transient signals", *IMA J. Math. Control and Information*, **1**, 117-128.

Goswami, I., Scanlan, R. H. and Jones, N. P. (1993a), "Vortex-induced vibrations of circular cylinders. I: experimental data", *J. Eng. Mech., ASCE*, **119**, 2270-2287.

Goswami, I., Scanlan, R. H. and Jones, N. P. (1993b), "Vortex-induced vibrations of circular cylinders. II: a new model", *J. Eng. Mech., ASCE*, **119**, 2288-2302.

Harlten, R. T. and Currie, I. G. (1970), "Lift-oscillator model of vortex-induced vibration", *J. Eng. Mech. Division*, *ASCE*, **96**(5), 577-591.

Hay, J. (1992), *Response of Bridge to Wind*, Transport Research Laboratory, Department of Transport, U.K. HMSO.

Iwan, W. D. and Blevins, R. D. (1974), "A model for vortex induced oscillation of structures", *J. Applied Mech.*, *ASME*, **41**, 581-586.

Law, S. S., Yang, Q. S. and Fang, Y. L. (2007), "Experimental studies on possible vortex shedding in the suspension bridge. Part II – Analysis results", *Wind Struct.*, 10(6), 555-576.

Petrovski, J. and Naumovski, N. (1979), *Processing of strong motion accelerograms. Part 1: Analytical methods.* Report 66. I211S, Stronjze.

Sarpkaya, T. (1978), "Fluid forces on oscillating cylinders", *J. Port, Coastal and Ocean Div., ASCE*, **104**(1), 19-24.

Simiu, E. and Scanlan, R. H. (1996), *Wind Effect on Structures*, John Wiley and Sons, New York, N.Y. 3rd. ed.

Skop, R. A. and Griffin, O. M. (1975), "On a theory for the vortex-excited oscillations of flexible cylindrical structures.", *J. Sound Vib*, **41**(3), 263-274.

Staubli, T. (1983), "Calculation of the vibration of an elastically mounted cylinder using experimental data from a forced oscillation", *J. Fluid Eng.,* **105**(2), 225-229.

Vickery, B. J. and Basu, R. I. (1983), "Across wind vibrations of structures of circular cross-section. Part II. Development of a mathematical model for full-scale application", *J. Wind Eng. Ind. Aerodyn.*, **12**, 49-73.

CC